

# QiR2017

by Dadan Ramdan

---

**Submission date:** 17-May-2021 09:19PM (UTC+0800)

**Submission ID:** 1587952732

**File name:** ber\_of\_Mold\_Cavity\_Vents\_on\_Wire\_Sweep\_in\_PBGA\_Encapsulation.pdf (590.43K)

**Word count:** 3798

**Character count:** 19568

UNIVERSITAS MEDAN AREA

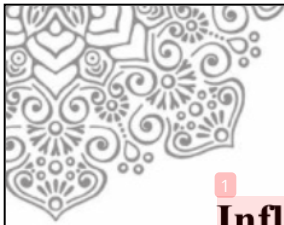
---

© Hak Cipta Di Lindungi Undang-Undang

Document Accepted 1/7/21

1. Dilarang Mengutip sebagian atau seluruh dokumen ini tanpa mencantumkan sumber
2. Pengutipan hanya untuk keperluan pendidikan, penelitian dan penulisan karya ilmiah
3. Dilarang memperbanyak sebagian atau seluruh karya ini dalam bentuk apapun tanpa izin Universitas Medan Area

Access From (repository.uma.ac.id)1/7/21



# Influence of Number of Mold Cavity Vents on Wire Sweep in PBGA Encapsulation: FSI-MpCCI Simulation

Dadan Ramdan, Darianto  
Mechanical Engineering Department  
Engineering Faculty, Medan Area University  
Medan, Indonesia  
dadan@uma.ac.id

ChuYee Khor, Mohd. Zulkifli Abdillah  
School of Mechanical Engineering  
Universiti Sains Malaysia  
Penang, Malaysia  
mezul@eng.usm.my

**Abstract**— This paper presents three-dimensional (3D) fluid structure interaction (FSI) technique; using Mesh based Parallel Code Coupling Interface (MpCCI), for the visualization of wire sweep during encapsulation of plastic ball grid array (PBGA) package. The effect of number of mold cavity vents on the melt flow behavior, wire sweep, and pressure and stress distributions, are mainly studied. The 3D model of mold and wires are created using GAMBIT, and the fluid flow and structure are simulated using FLUENT and ABAQUS, integrated with MpCCI. The Castro-Macosko model is used to incorporate the polymer rheology and Volume of Fluid (VOF) technique is applied for melt front tracking. User-defined functions (UDFs) are incorporated to allow for curing kinetics. Wire sweep profiles and pressure distribution around wires region within the mold are presented. The numerical results of melt front patterns and filled volume are compared with the previous experimental results and found in good agreement. It is observed that the number of vents significantly influence the pressure force developed inside the mold cavity and the eventual wire sweep; as the number of vents increases, wire sweep decreases.

**Keywords**— fluid structure interaction; mesh based parallel code coupling interface; Castro-Macosko model; Epoxy molding compound; Volume of fluid; Wire sweep.

## I. INTRODUCTION

The continuous reduction of chip size in the modern electronic industry has a significant impact on circuit design and assembly process of IC packages. Reduced chip size with increased I/O counts result in serious wire deflection during transfer molding process. If the deformation of wire is too large, it can cause a short circuit due to touching of adjacent wires or open circuit due to wire breakage [1]. Wire sweep has been recognized as one of the major defects in the encapsulation of microelectronic chips by the transfer molding process [2], [3]. The prediction of wire sweep during encapsulation involves coupled solution of mold flow and structural deformation of wires, making it a typical fluid-structure interaction (FSI) problem [4], [5]. Many researchers have focused on this issue using various computational Computer-aided engineering (CAE) techniques.

In all the previous works on wire sweep prediction, the fluid and structural solvers were run separately and coupled

manually. As a promising breakthrough in the FSI analysis, the Mesh based parallel Code Coupling Interface (MpCCI) technique has recently been introduced for the simultaneous real time coupling of fluid and structural solvers. The use of a finite volume flow solver and a finite element structural solver, coupled through MpCCI was reported for variety of engineering problems [6] – [8]. However, as far as the authors are aware, the use of MpCCI for wire sweep analysis and the study on the effect of number of vents on wire deformation during the encapsulation of plastic ball grid array (PBGA) package have not been reported so far. To address this problem, the finite-volume flow solver FLUENT and the finite-element structural solver ABAQUS are interfaced by MpCCI. Polymer rheology model with curing effect (Castro-Macosko model) is used in the fluid flow model and VOF technique is applied for melt front tracking of the EMC. The numerical analysis uses User-defined functions (UDFs) to account for curing kinetics. Keeping one gate, three configurations of mold cavity with 2, 4 and 6 vents are simulated. Melt front profiles, wire sweep, pressure field, and stress distribution on wires, are analyzed for each case. The proposed model is well validated by the published experimental results of Yang *et al.*, (2000) [9].

## II. MATHEMATICAL MODEL

### A. Fluid Flow Analysis

In the simulation model, the encapsulation process material and air are assumed incompressible and the governing equations describing the fluid flow are conservation of mass, conservation of momentum, and conservation of energy [10]. FLUENT normally solves the governing equations using Cartesian spatial coordinates and velocity components.

The conservation of mass or continuity equation is:

$$\frac{\partial \rho}{\partial t} + \frac{\partial}{\partial x_i}(\rho u_i) = 0 \quad (1)$$

Eq. (1) is the general form of the mass conservation equation and is valid for incompressible and compressible flows. Conservation of momentum in  $i^{\text{th}}$  direction in an inertial (non accelerating) reference frame is described by:



$$\frac{\partial}{\partial t}(\rho u_i) + \frac{\partial}{\partial x_i}(\rho u_i u_i) = -\frac{\partial p}{\partial x_i} + \frac{\partial \tau_{ij}}{\partial x_j} + \rho g_i + F_i \quad (2)$$

where,  $P$  is the static pressure,  $\tau_{ij}$  is the viscous stress tensor and  $g_i$  and  $F_i$  are the gravitational acceleration and external body force in the  $i$  direction, respectively.

The energy equation cast in terms of  $h$  (static enthalpy) can be written as,

$$\frac{\partial}{\partial t}(\rho h) + \frac{\partial}{\partial x_i}(\rho u_i h) = \frac{\partial}{\partial x_i}(k \frac{\partial T}{\partial x_i}) + \eta \dot{\gamma} \quad (3)$$

where  $T$  is the temperature,  $k$  is the thermal conductivity,  $\eta$  is the viscosity and  $\dot{\gamma}$  is the shear rate. The molding compound was assumed to be a generalized Newtonian fluid (GNF).

Several models have been used to predict the relationship between viscosity and the degree of polymerization. The Castro-Macosko model has been applied in encapsulation process [8] and is selected to use in this simulation. It can be described as follows:

$$\mu(T, \dot{\gamma}) = \frac{\mu_0(T)}{1 + (\frac{\mu_0(T)}{\tau^*})^{1-n}} (\frac{\alpha_g}{\alpha_g - \alpha})^{C_1 + C_2 \alpha} \quad (4)$$

where  $n$  is the power law index,  $\mu_0$  the zero shear rate viscosity,  $\tau^*$  is the parameter that describes the transition region between zero shear rates and the power law region of the viscosity curve,  $\dot{\gamma}$  is the shear rate,  $\alpha$  is the conversion,  $\alpha_g$  is the conversion at the gel point and  $C_1$  and  $C_2$  are fitting constants.

$$\mu_0(T) = B \exp\left(\frac{T_b}{T}\right) \quad (5)$$

$B$  is an exponential-fitted constant and  $T_b$  is a temperature fitted-constant. In addition, Kamal curing kinetics is coupled together with Castro-Macosko model. This model predicts the rate of chemical conversion of the compound as follows:

$$\frac{d\alpha}{dt} = (k_1 + k_2 \alpha^{m_1})(1 - \alpha)^{m_2} \quad (6)$$

and

$$k_1 = A_1 \exp\left(-\frac{E_1}{T}\right) \quad (7)$$

$$k_2 = A_2 \exp\left(-\frac{E_2}{T}\right) \quad (8)$$

where  $\alpha$  is the conversion,  $A_1$  and  $A_2$  are the Arrhenius pre-exponential factors,  $E_1$  and  $E_2$  are the activation energies,  $m_1$  and  $m_2$  are the reaction orders and  $T$  is the absolute temperature. TABLE I summarized the material properties of the EMC considered in the current study.

The basic idea of the VOF scheme is to locate and evolve the distribution of, say, the liquid phase by assigning for each cell in the computational grid a scalar,  $f$ , which specifies the fraction of the cell's volume occupied by liquid. Thus,  $f$  takes

the value of 1 ( $f = 1$ ) in cell which contains only resin, the value 0 ( $f = 0$ ) in cells which are void of resin, and a value between 0 and 1 ( $0 < f < 1$ ) in "interface" cells or referred as the resin melt front. The equation of melt front over time is governed by the following transport equation:

$$\frac{\partial f}{\partial t} + \nabla \cdot (uf) = 0 \quad (9)$$

TABLE I. EMC MATERIAL PROPERTIES [11].

	Parameter	Value	Unit
Castro Macosko Model	$\alpha_g$	0.17	-
	$B$	0.000381	Kg/m/s
	$T_b$	5230	K
	$n$	0.7773	-
	$\tau$	0.0001	N/m <sup>2</sup>
	$C_1$	1.03	-
	$C_2$	1.50	-
Curing Kinetics	$m_1$	1.21	-
	$m_2$	1.57	-
	$A_1$	33530	1/s
	$A_2$	30540000	1/s
	$E_1$	7161	K
	$E_2$	8589	K
	$\alpha$	0.05	-
Density	$\rho$	2000	Kg/m <sup>3</sup>
Specific Heat	$C_p$	1079	J/Kg-K
Thermal Conductivity	$k$	0.97	W/m-K
Reference Temperature	$T$	298	K

## B. Wire Sweep Analysis

To calculate the drag force exerted on the wires by the resin flow, the value of velocities and viscosities have to be determined from the mold filling simulation. The effect of wire density on the resin flow is considered according to their occupied volume in the three dimensional filling simulation. Then, the Lamb's model is utilized to calculate the drag force as follows [1]:

$$D = \frac{C_D \rho U^2 d}{2} \quad (10)$$

where  $D$  is the drag force per unit length,  $\rho$  is the fluid density,  $U$  is the undistributed upstream velocity,  $d$  is the wire diameter and  $C_D$  is the drag coefficient, which can be written as:

$$C_D = \frac{8\pi}{Re[2.002 - \ln(Re)]} \quad (11)$$

where  $Re$  is the Reynold number, which can be defined as:

$$Re = \frac{\rho u d}{\eta} \quad (12)$$

where  $\eta$  is the fluid viscosity.

Wire sweep deflection  $\delta$  can be written as [12]:

$$\delta_{max} = S * D \left( f_B \left( \frac{H}{L} \right) \frac{H^3}{EI} + f_T \left( \frac{H}{L} \right) \frac{L^3}{GI_p} \right) \quad (13)$$

where  $S$  is the length of the wire bond,  $f_B$  is the bending geometry factor for the bending moment,  $f_T$  is the twisting geometry factor for the twisting moment,  $H$  is the height of wire,  $L$  is the length of wire span,  $G$  is the shear modulus of wire,  $E$  is the elastic modulus of wire,  $I$  is the momentum of inertia of the wire,  $I_p$  is the polar momentum of inertia of the wire.

### III. SIMULATION MODEL

#### A. Simulation Model and Boundary Conditions in FLUENT

The volume of fluid (VOF) model in FLUENT 6.3.26 is utilized to simulate the process [13] – [15]. In the VOF model, a single set of momentum equations is shared by the fluids, and the volume fraction of each of the fluids in each computational cell is tracked throughout the domain [15]. Air and EMC are defined as the phases in the analysis. Implicit solution and time dependent formulation are applied for the volume fraction in every time step. The volume fraction of the encapsulation material is defined as one and zero value for air phase.

The Castro-Macosko viscosity model with curing effect was written into C language using Microsoft VISUAL Studio 2005 and compiled as UDF in FLUENT. The mold cavity package models with different number of vents, and its boundary conditions are shown in Fig. 1. The dimension of mold cavity is 100 mm × 100 mm × 5 mm, die is 30 mm × 30 mm × 1mm and inlet is 8 mm × 8 mm [16]. The flow direction is diagonal of x and z direction to the un-deformed wire axis and the properties are approximately the same as those used in ref. [16]. The model is created by using GAMBIT software and average 395,000 tetrahedral elements are generated for simulation (Fig. 2) in terms of accuracy and computational cost. Besides, time step size is also tested and 0.001 s is found to be the optimum. The governing equations are discretized by the first order upwind scheme, and solved by SIMPLE algorithm.

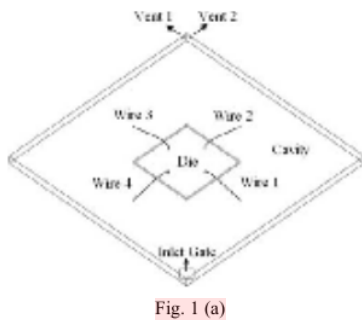


Fig. 1 (a)

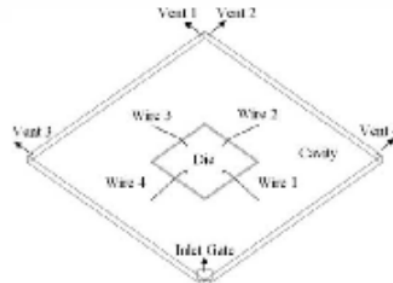


Fig. 1 (b)

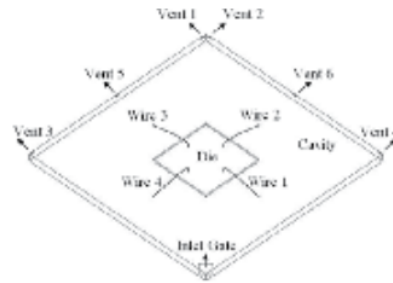


Fig. 1 (c)

Fig. 1. Mold cavity models with: (a) 2 vents (b) 4 vents and (c) 6 vents.

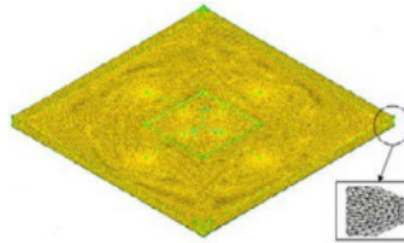


Fig. 2. Meshed model with 2 vents for FLUENT analysis.

The boundary and initial conditions used in the calculation are as follows [15]:

- On wall :  $u = v = w = 0$ ;  $T = T_w$ ;  $\frac{\partial p}{\partial n} = 0$
- On centre line :  $\frac{\partial u}{\partial y} = \frac{\partial v}{\partial y} = \frac{\partial w}{\partial y} = \frac{\partial T}{\partial y} = 0$
- On melt front :  $p = 0$
- At inlet :  $u = u_{in}(x,y,z)$ ;  $T = T_{in}$

The mold temperature was considered as 175°C and the package inlet velocity was 0.6 m/s. The simulation is performed on an Intel Core 2 Duo processor E7500, 2.93 GHz with 2 GB of RAM; it took around 74 hours for each case to complete 15,000 iterations in time steps of 0.001s.

#### B. The computational domain and boundary conditions in ABAQUS

Commercial FEM based software; ABAQUS is used in this study to calculate the wire deformation. The structures of the wires are imported from GAMBIT in ACIS '.sat' format. The dimensions of the gold wire used in this study are chosen according to the model of Yang *et al.*, (2000). The wire (Fig. 3) has a span,  $L = 20$  mm, height  $H = 3.5$  mm and diameter  $d = 0.14$  mm. The wire is divided into 10,191 tetrahedral elements as shown in Fig. 4. The shape of the wire is also classified as typical Q-auto loop wire [17]. The ball bond boundary conditions of wire are set as fixed in ABAQUS and shown in Fig. 5. The wire mechanical properties are as follows: elastic modulus,  $E=50$  GPa [18], density,  $\rho=1800$  kg/m<sup>3</sup>, Poisson's ratio,  $\nu = 0.42$  and reference temperature,  $T=175^\circ\text{C}$ .

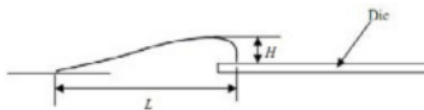


Fig. 3. Wire specifications.

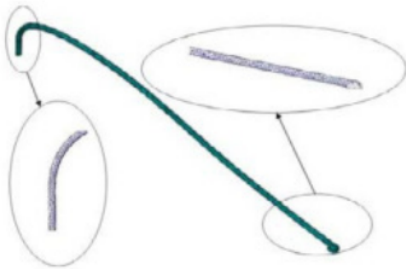


Fig. 4. Meshed wire for ABAQUS analysis.

#### C. Mesh based Parallel Coupling Code Interface (MpCCI)

MpCCI is a software library which enables the exchange of data defined on meshes of two or more simulation codes in the coupling region. Since the meshes need not match point by point, MpCCI performs an interpolation and, in case of parallel codes, keeps track of the distribution of the domains onto different processes [7]. In this way, the intricate details of the data exchange are hidden behind the concise interface of MpCCI. As a consequence, the simulation codes themselves

are changed only moderately when they are prepared for coupling via MpCCI (Fig. 6).

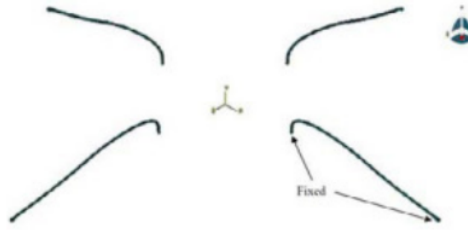


Fig. 5. Boundary condition of wires in ABAQUS [19].

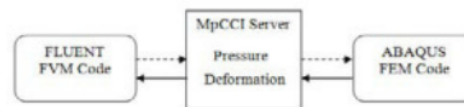


Fig. 6. FLUENT and ABAQUS coupling simulation process [20].

### IV. RESULT AND DISCUSSION

#### A. Model Validation

The present simulation results of fluid flow (for 2 vents case) are validated with the experimental results of Yang *et al.*, (2000) [9] who investigated the flow behavior of epoxy resin (D.E.R.331, Dow Chemical). Fig. 6 shows the comparison of predicted and experimental flow profiles of the PBGA encapsulation process from 4 to 10 s of filling. The simulation results show separate profiles for wire sweep and EMC filling, at various stages of filling. The predicted EMC flow profiles show good agreement with the experimental results, at all time steps. Wire displacement phenomenon is observed when the EMC flow around the wire region. The EMC volume versus filling time for the simulation and the experiment is also plotted and compared as in Fig. 7; the maximum discrepancy is found about 6.7 %.

Further, the wire deformation is validated with analytical method proposed by Kung *et al.* (2006) [21]. The comparison of simulation and analytical results [21] of wire deformation for wire 4 in x-direction is shown in Fig. 8. The analytical calculation refers to eq. (13) with  $f_b = 0.165$ ,  $f_r = 0.00165$  and  $H/L = 0.175$ . The average deviation at maximum displacement (after 9 s) is found to be 6.5 %. The results demonstrate good quantitative agreement.

#### B. Melt Front Profile

First of all the effect of number of vents on the melt front profile is visualized for various stages of filling, as presented

in Fig. 9. It is observed that the melt flow pattern follows almost similar trend in all the cases; this indicates that the melt front advancement is not significantly influenced by the number of vents.

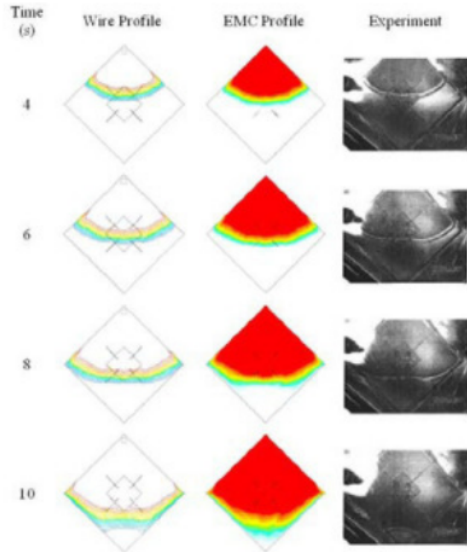


Fig. 6. Comparison of simulation and experiment [9] for wire deformation and EMC flow profiles (2 vents case).

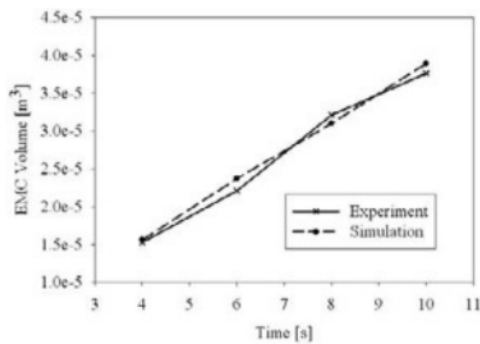


Fig. 7. Comparison of EMC filled volume for experiment [9] and simulation (2 vents case).

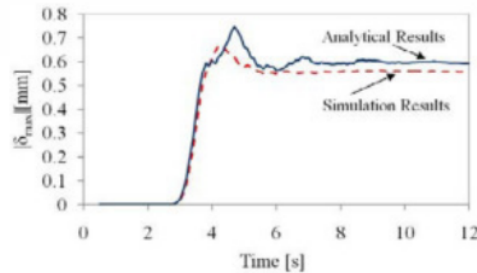


Fig. 8: Comparison simulation and analytical results [21] of wire deformation for wire 4 in x-direction (2 vents case).

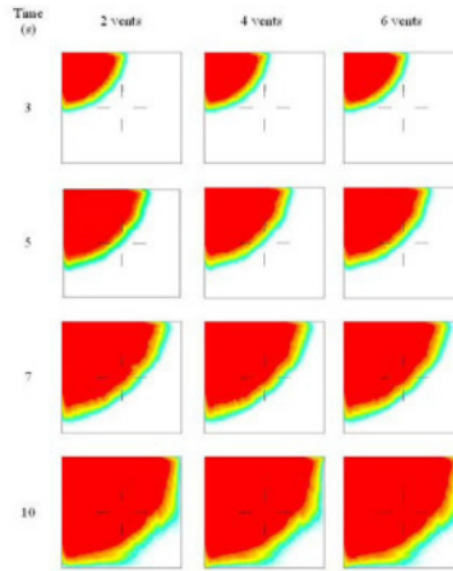


Fig. 9. Melt front profiles of three cases at various filling stages.

### C. Wire sweep

Fig. 10 illustrates the phenomenon of wire deformation, predicted by ABAQUS. The magnitude of wire deformation for each wire is also estimated and plotted as shown in Fig. 11. It is clear that the wires 1 and 4 are significantly deformed compared to wires 2 and 3, in all the cases. At the same time, it is worth noting that, as the number of vents increases, the sweep tendency decreases, presumably due the reduced pressure force inside the cavity.

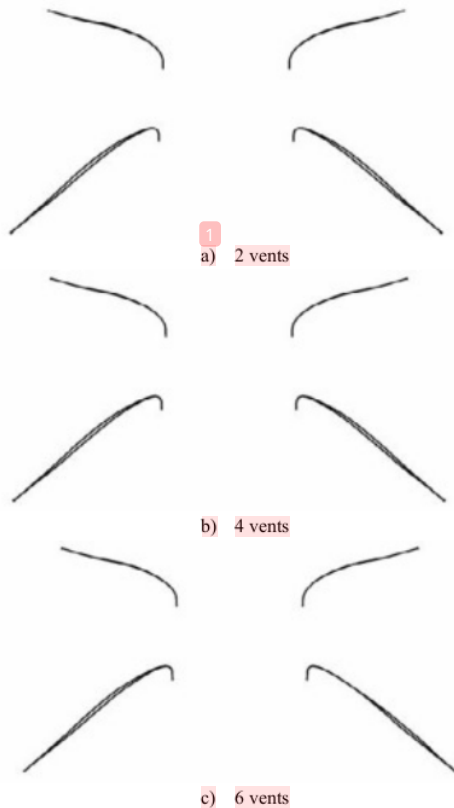


Fig. 10: Illustration of wire sweep predicted by ABAQUS.

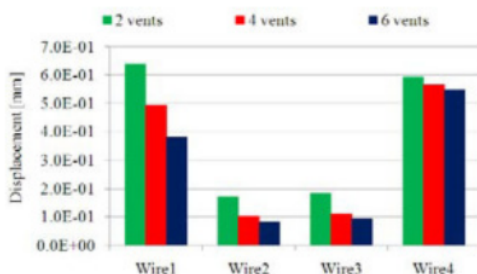


Fig. 11: Comparison of deformation of wires 1-4 for all the cases.

#### D. Void occurrence

It has been shown in the previous sections that increasing the number of vents could reduce the wire sweep. However, it would be interesting to study the limiting factors of increasing the vents for a given mold cavity and number of gate. Thus in the present study, an attempt is also made to observe how the number of vents influence the development of voids during the encapsulation process. Fig. 12 shows the melt front profiles showing the void locations for various cases, and Fig. 17 shows the graphical comparison of the respective percentages of voids. It is observed that, as the number of vents increases, the void formation increases significantly; this apparently imposes restriction on the number of vents. However, as is clear from Fig. 16, since the voids are situated near the walls, and the wire zone is not affected, the increased number of vents does not presumably pose significant threat on the quality of mold filling.

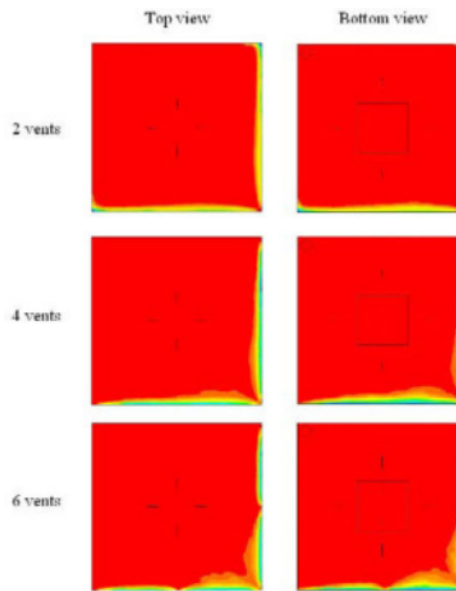
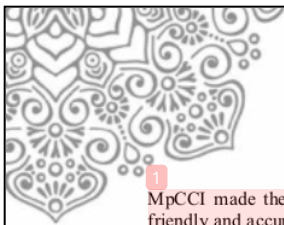


Fig. 12: Mold filling contours for various cases after 15s, showing voids.

#### V. CONCLUSION

The coupled three dimensional FLUENT-ABAQUS-MpCCI facility was successfully employed to study the effect of number of vents on wire sweep during the encapsulation of a typical PBGA package. The major contributions in this work are the use of MpCCI, and the investigation of the effect of number of vents on wire sweep. Unlike the conventional manual coupling of flow and structural simulations, the



MpCCI made the present FSI analysis more effective, user-friendly and accurate. The wire sweep and melt front profiles were compared with the previous experimental results and found in good agreement. It was observed that the number of vents had crucial influence on wire sweep which decreased with increase of vents. Further, the analysis of Von-Mises stress showed that the potential fracture of wires due to excessive stresses could be eliminated by the increase of number of vents. This study may be improved by considering the optimization of number of gates and vents, and their locations. Precise experiment on realistic packaging environment is also recommended to substantiate the present predictions.

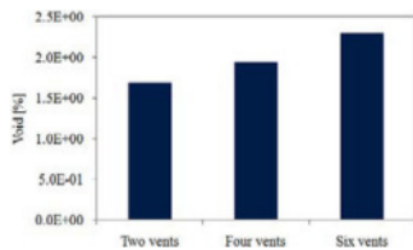


Fig. 17: Voids percentage in various cases after 15s.

#### ACKNOWLEDGMENT

The authors gratefully acknowledged the Intel Tech. Sdn. Bhd., Penang for the financial support of this research work. The author would also like to thank DGHE National Education and Culture Department of Republic of Indonesia for Research Found of PHB skim in 2016 FY. Lastly, the author would also like to thank C.Y. Khor for the technical software advices in the present study.

#### REFERENCES

- [1] J. Su, S. J. Hwang, F. Su, S. K. Chen, "An Efficient Solution for Wire Sweep Analysis in IC Packaging," *J. Electron. Packag.*, ASME, vol. 125, pp. 139-143, March 2003.
- [2] W. R. Jong, Y. R. Chen, T. H. Kuo, "Wire Density in CAE analysis of high pin-count IC packages: Simulation and verification," *Int. Commun. Heat and Mass Transfer*, vol. 2, pp. 1350-1359, 2005.
- [3] M. S. Rusdi, M. Z. Abdullah, A. S. Mahmud, C. Y. Khor, M. S. Abdul Aziz, Z. M. Ariff, M. K. Abdullah, 2016, Numerical Investigation on the Effect of Pressure and Temperature on the Melt Filling During Injection Molding Process, *Arab J Sci Eng* (2016) 41:1907–1919, DOI 10.1007/s13369-016-2039-0.
- [4] C.Y. Khor, M.Z. Abdullah, Chun-Sean Lau, I.A. Azid, 2014, Recent fluid-structure interaction modeling challenges in IC encapsulation – A review, *Microelectronics Reliability* 54 (2014) 1511–1526.
- [5] C.Y. Khor, Muhammad Ikman Ishak, M.U. Rosli, Mohd Riduan Jamaludin, M.S. Zakaria, A.F.M. Yamin, M.S. Abdul Aziz, and M.Z. Abdullah, 2017, Influence of Material Properties on the Fluid Structure Interaction aspects during Molded Underfill Process, *MATEC Web of Conferences* 97, 01059 (2017) *ETIC 2016*, DOI: 10.1051/mateconf/20179701059.
- [6] S. Yigit, M. Schafer, M. Heck, "Grid movement techniques and their influence on laminar fluid-structure interaction computations," *J. Fluids and structures*, Vol. 24, pp. 819-832, 2008.
- [7] F. Thirifay and P. Geuzaine, "Numerical simulations of fluid-structure interaction problem using MpCCI," address: <http://citeseerx.ist.psu.edu/viewdoc/download>, 2008.
- [8] B. Gatzhammer, M. Mehl, T. Neckel, "A coupling environment for partitioned multiphysics simulations applied to fluid-structure interaction scenarios," *Procedia Comput. Science*, Vol. 1, pp.681-689, 2010.
- [9] Yang S.-Y., Jiang S.-C., and Lu W.-S. (2000), "Ribbed package geometry for reducing thermal warpage and wire sweep during PBGA encapsulation", *IEEE Transactions on Components and Packaging Technologies*, Vol. 23, No.4, pp. 700-706.
- [10] D. Ramdan, M. Z. Abdullah, C. Y. Khor, "Plastic Ball Grid Array Encapsulation Process Simulation on Rheology Effect," *TELKOMNIKA*, vol. 9, no. 1, pp. 27–36, April 2011.
- [11] L. Nguyen, C. Quentin, W. Lee, S. Bayyuk, S. A. Bidstrup-Allen, S. T. Wang, "Computational Modeling and Validation of the Encapsulation of Plastic Packages by Transfer Molding," *Trans. of the ASME*, vol. 122, pp. 138-146. 2000.
- [12] H. K. Kung, J. N. Lee, C. Y. Wang, "The Wire Sweep Analysis Based on the Evaluation of the Bending and Twisting Moments for Semiconductor Packaging," *Microelectron. Eng.* 83, pp. 1931-1939, 2006.
- [13] Khor C.Y., Abdullah M.Z., Abdullah M.K., Muijebu M.A., Ramdan D., Majid M.F.M.A., Ariff Z.M., Abdul Rahman M.R. (2011), "Numerical analysis on the effects of different inlet gates and gap heights in TQFP encapsulation process", *Int. J. of Heat and Mass Transfer*, Vol. 54, pp. 1861-1870.
- [14] Khor C.Y., Abdullah M.K., Abdullah M.Z., Abdul Muijebu M., Ramdan D., Majid M.F.M.A., Ariff Z.M. (2010)-(a), "Effect of vertical stacking dies on flow behavior of epoxy molding compound during encapsulation of stacked-chip scale packages", *Heat and Mass Transfer*, Vol. 46, pp. 1315-1325.
- [15] Khor C.Y., Abdul Muijebu M., Abdullah M.Z., Che Ani F. (2010)-(b), "Finite volume based CFD simulation of pressurized flip-chip underfill encapsulation process", *J. of Microelectronics Reliability*, pp. 98-105.
- [16] Han S.-J. and Huh Y.-J. (2000), "A study of wire sweep during encapsulation of semiconductor chips", *J. of the Microelectronics and Packaging Society*, Vol. 7, No. 4, pp. 17-22.
- [17] J. M. Brand, S. A. Ruggero, A. J. Shah, "Wire sweep Reduction via Direct Cavity Injection During Encapsulation of Stacked Chip-Scale Packages," *J. Electron. Packag.*, Vol. 130, pp. 011011-1 – 011011-6, March 2008.
- [18] Yang W.-H., Hsu D.C., Yang V., Chang R.-Y., Su F., Huang S.-J. (2004), *Three dimensional CAE of wire-sweep in microchip encapsulation*, Technical Conference-ANTEC, Conference Proceeding, Vol.2, pp. 1679-1683.
- [19] D. Ramdan, U. Harahap, A. Rubiantara, C. Y. Khor (2016), Fluid Structure Interaction Numerical Simulation of Wiresweep in Electronics Packaging, *TELKOMNIKA*, vol. 14, no. 1, pp. 262 – 272, March 2016.
- [20] MpCCI 3.1.0-1 Documentation part I overview, Fraunhofer Institute for Algorithms and Scientific Computing SCIA, Germany, January 2009.
- [21] Kung H.-K., Lee J.-N., Wang C.-Y. (2006), "The wire sweep analysis based on the evaluation of the bending and twisting moments for semiconductor Packaging", *Microelectronic Engineering*, Vol. 83, pp. 1931-1939.

**95%**  
SIMILARITY INDEX

**95%**  
INTERNET SOURCES

**68%**  
PUBLICATIONS

**%**  
STUDENT PAPERS

### PRIMARY SOURCES

1	<a href="http://eprints.undip.ac.id">eprints.undip.ac.id</a> Internet Source	89%
2	<a href="http://repository.uma.ac.id">repository.uma.ac.id</a> Internet Source	3%
3	Dadan Ramdan, Usman Harahap, Mohd. Zulkifli Abdillah. "Fluid structure interaction simulation in IC encapsulation process", 2013 International Conference on QiR, 2013 Publication	2%
4	C.Y. Khor, M.Z. Abdullah, M.K. Abdullah, M.A. Mujeebu, D. Ramdan, M.F.M.A. Majid, Z.M. Ariff, M.R. Abdul Rahman. "Numerical analysis on the effects of different inlet gates and gap heights in TQFP encapsulation process", International Journal of Heat and Mass Transfer, 2011 Publication	1%
5	<a href="http://core.ac.uk">core.ac.uk</a> Internet Source	<1%

---

Exclude quotes	Off
Exclude bibliography	Off

Exclude matches	Off
-----------------	-----

FINAL GRADE

/0

GENERAL COMMENTS

Instructor

PAGE 1

PAGE 2

PAGE 3

PAGE 4

PAGE 5

PAGE 6

PAGE 7